

## Preparation And Characterisation Of ZnO Thin Films Deposited By SILAR Method

A. Raidou<sup>a</sup>, M. Aggour<sup>a</sup>, A. Qachaou<sup>a</sup>, L. Laanab<sup>b</sup>, M. Fahoume<sup>a</sup>

<sup>a</sup> L.P.M.C., Faculté des Sciences, Université Ibn Tofail, BP.133-14000 Kénitra, Morocco

<sup>b</sup> L.C.S., Faculté des Sciences, université Mohammed V, BP.1014 Rabat, Morocco

**Abstract:** Zinc oxide (ZnO) thin films were grown on glass and copper substrates by the Successive Ionic Layer Adsorption and Reaction (SILAR) technique.

ZnO films are obtained by successive immersion of a substrate in an aqueous solution containing: ZnSO<sub>4</sub> with different molarities, 6ml/100ml 13.15 M aqueous ammonia solution and in deionised water heated at different temperatures.

We studied the structural, morphological and optical properties with the deposition parameters (pH, bath temperature, number of cycles...)

The structural, morphological surface and optical properties of the films have been studied by using X-ray diffraction (XRD), scanning electron microscopy (SEM) and UV-VIS-spectrophotometer. Effects of experimental parameters and heat treatment on the structural and optical properties were discussed. The X-ray diffraction analysis shows that the films are polycrystalline with zincite hexagonal structure with the preferential orientation of (002) plan.

The study of surface morphology reveals that deposited ZnO films take many shapes: nanorods, nanoprisms, flower-like, needles, spindles and hexagonal structures. Obtained ZnO films exhibit a high transmittance of 90% in visible band, and optical band gap of 3.27 eV.

### I. Introduction

Semiconductor thin films are always important in materials science due to their outstanding electrical and optical properties, which are useful in various optoelectronic devices. zinc oxide (ZnO) is an interesting wide band gap (~3.3 eV) II-VI semiconductor because exhibits numerous characteristics suited for various technological applications such as antireflection coatings, transparent electrodes in solar cells [1], piezoelectric devices [2], gas sensors [3], varistors [4], UV and blue light emitters [5] and even thin film transistors [6]. Various chemical and physical processes have been employed for thin film deposition, such as conventional sputter deposition technique [7], chemical vapor deposition (CVD) [8,9], thermal evaporation [10,11], spray pyrolysis [12,13], and electrodeposition [14]. Like chemical bath deposition technique, the Successive Ionic Layer Adsorption and Reaction (SILAR) technique for the preparation of thin films from aqueous solution is a promising technique because of its simplicity and economics. The facts affecting the process are the quality of the precursor solutions, their concentrations, pH values, complexing agents and individual rinsing and immersion time periods [15].

### II. Experimental

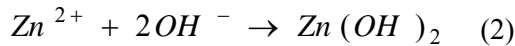
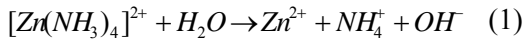
The ZnO thin films were prepared by successive immersion of copper and clean glass substrates (75

mm x 25 mm x 1mm). It is noteworthy that any substrates can be used where main criteria in the selection is that the selected substrates do not react with the bath precursor solutions. Using the same method, Jimenez-Gonzalez and co-workers [16,17] have prepared the ZnO films and studied their photosensitivity. First in a dilute solution of zinc amine complex (0.04 M to 0.08 M Zinc sulphate and 6ml/100ml 13.15 M aqueous ammonia solution) and in distilled water heated to a temperature determined. The crystal structure was determined with a XPERT-PRO PW-3064 X-ray diffractometer using Cu K $\alpha$  ( $\lambda = 1.540598 \text{ \AA}$ ). The optical characterization of the films was done by Perkin Elmer Instrument lambda 900 UV/Vis/NIR spectrophotometer.

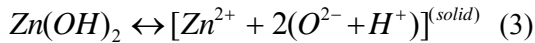
### III. Experimental results and discussion

The SILAR method is mainly based on the adsorption and reaction of the ions from the solution and rinsing between every immersion with deionised water to avoid homogeneous precipitation in the solution. The SILAR is based on sequential reaction at the substrate surface. In general, the SILAR growth cycle contains four different steps: adsorption, rinsing, reaction and rinsing. Rinsing follows each reaction, which enables heterogeneous reaction between the solid phase and the solvated ions in the solution.

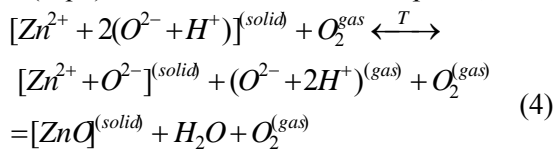
The deposition of ZnO thin films on glass slides, silicon and copper substrates at different temperatures was achieved using 100 ml of zinc sulfate and 6ml/100ml 13.15 M aqueous ammonia solution as precursor solution. The pH was adjusted by KOH addition. In the first step, the substrate was immersed in a beaker containing  $Zn(SO_4)$  and ammonia solution, where  $Zn^{2+}$  with ammonia formed zinc ammonia complex  $[Zn(NH_3)_4]^{2+}$ . In the first immersion process, zinc ammonia was adsorbed onto the substrate. In the second step, the zinc ammonia adsorbed substrate was immersed into beaker containing the distilled water, where the adsorbed zinc ammonia complex was converted into zinc hydroxide  $(Zn(OH)_2)$ . Each immersion step took a time period of 30 s. the detailed chemical reactions involved in the SILAR growth process are given as follows



In order to consider the transformation of the hydroxide phase during the heat treatment,  $Zn(OH)_2$  could be written in a equivalent form, in the Kofstad notation [18,19]



At higher temperature in air atmosphere, the hydroxide phase (Eq.3) is transformed into oxide phase,



### III-1. Structural analysis

Fig. 1 shows XRD patterns of ZnO thin films deposited at different pH values (10.6, 11.8 and 12) on

glass substrates, and annealed at 450 °C for 2 h. It is found that the pH plays an important role in determining the crystal structure of ZnO thin films. The XRD patterns has shows three peaks close to  $2\theta=31.758^\circ$  ( $d_{100}=2.927\text{\AA}$ ),  $34.432^\circ$  ( $d_{002}=2.7246\text{\AA}$ ) and  $36.303^\circ$  ( $d_{101}=2.6021\text{\AA}$ ) are attributed to the (100), (002) and (101) planes respectively of hexagonal ZnO, as can be seen in comparison with the ASTM card. In

particular, it was clearly observed the  $\frac{I(100)}{I(002)}$  ratio

increase with increasing pH. Therefore, the increase in pH promotes the preferential orientation (100). In contrast, no deposition of ZnO films were observed for pH values less than 9.

We also deposited the ZnO thin films on copper substrates, and annealed at 450 °C for 2h. Its spectra reveal the same three peaks of ZnO thin films described previously. Two strong peaks correspond to the copper substrates. And in addition, we observe two peaks of copper oxide (CuO) which are due to the contamination of the copper substrates during heat treatment. It was observed that the deposition of ZnO thin films on copper substrates present a preferential orientation (002).

Analysis of the calculated d-spacing on the basis of hexagonal structure can be made by means of the corresponding equation

$$d_{hkl} = \frac{1}{\sqrt{\frac{4}{3} \frac{h^2 + hk + k^2}{a^2} + \frac{l^2}{c^2}}} \quad (5)$$

Where  $h$ ,  $k$ , and  $l$  are the Miller indexes,  $a$  and  $c$  are lattice parameters. The values calculated for  $a$  and

$c$  are  $3.3798 \text{ \AA}$  and  $5.4492 \text{ \AA}$  ( $\frac{c}{a} = 1.6123$ ),

respectively, in agreement with lattice constants of ZnO zincite phase existing in the literature of ASTM card:  $a=3.2648\text{\AA}$  and  $c=5.2194 \text{ \AA}$ .

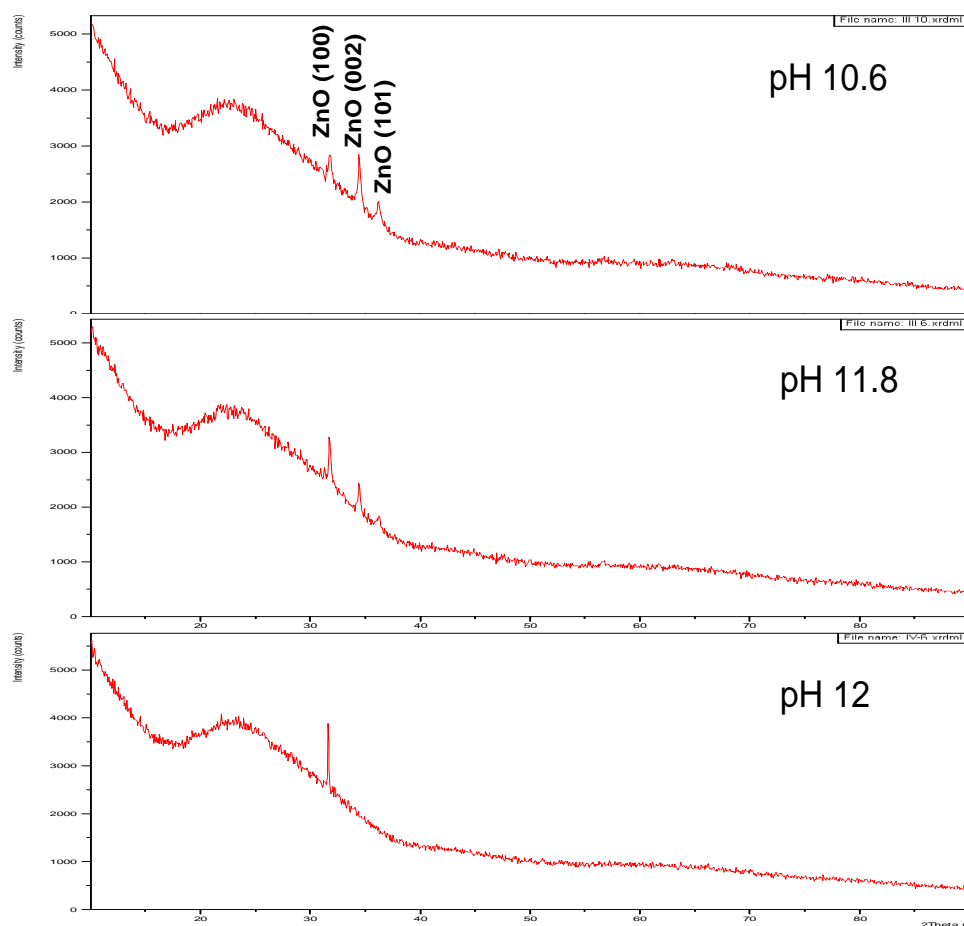


Fig. 1. X-ray diffraction spectra of ZnO films deposited on glass substrates in the same conditions: bath temperatures 80 °C, immersion time 30 s, number of cycles 20 and different pH values ( 10.6, 11.8 and 12) with an annealing temperature 450°C.

### III-2. Surface morphology

The surface morphological studies of the ZnO films have been carried out from scanning electron micrographs (SEM). Fig. 2 shows the SEM images of two ZnO films deposited, on copper substrates, in the same conditions and at two different pH values 11.6 and 12.2, and annealed at 450 °C for 2h. From the Fig. 2(a), it is observed that the zinc oxide wurtzite structure prepared at pH 11.6 is obtained in the form of needles, which takes different and random directions. Fig. 2(b) reveals that the ZnO thin films obtained at pH 12.2 is compact and relatively not dense. The structure of this film is hexagonal whose c-axis is perpendicular to the surface. Via the study of surface morphology, we have found that the gains of ZnO films take other shapes, which are also found by other

authors, like: spindles[20], nanorods [21,22], nanoprisms [23], nanotubes [24], flower-like [25,26] and needles [27]. It was concluded that the morphology of ZnO structure changes following the preparation parameters (bath temperature, molarity, pH...). The effect of annealing has been studied, we note that the annealing promotes the expansion of the grain size, and we also observed, at high heat treatment (550 °C) the posting of films deposited on copper substrates.

EDAX spectrum shows the existence of the constituent atoms (oxygen and zinc) of our film (Fig. 2.b), and the absence of impurities. The percentage of these atoms confirms a good stoichiometry (52.48 at. % O and 47.52 at. % Zn).

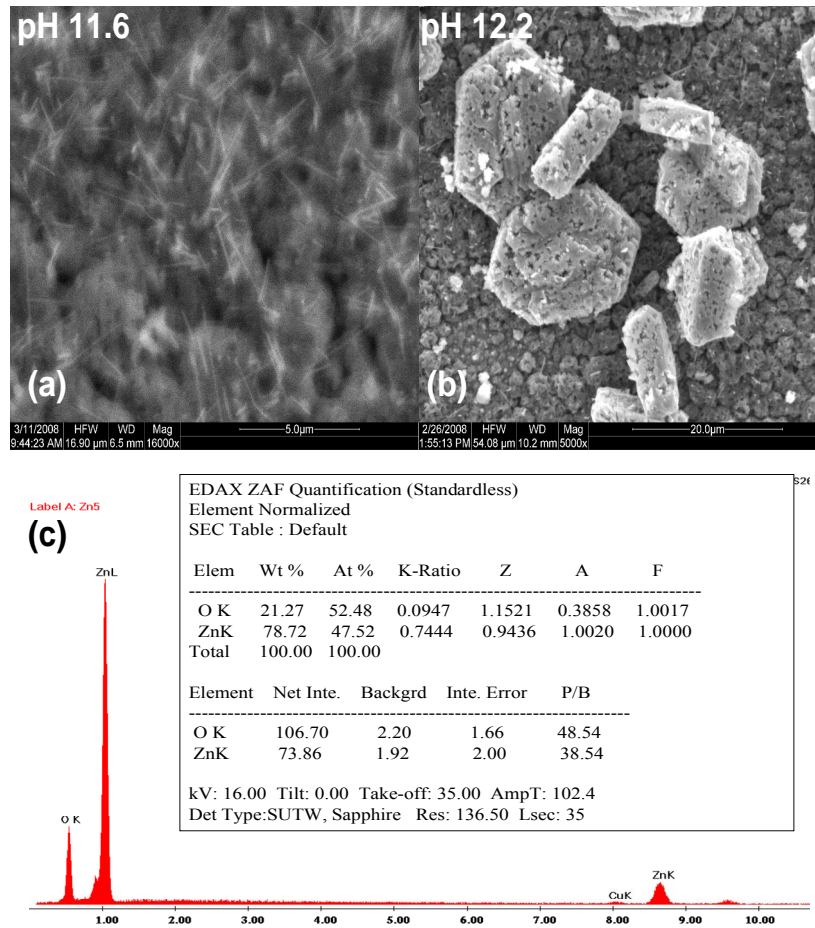


Fig. 2. SEM micrographs of ZnO films deposited on copper substrates in the same conditions: bath temperatures 80 °C, immersion time 30 s, number of cycles 40, annealing temperature 450°C, and two different pH values (a) 11.6 and (b) 12.2 with his EDAX spectrum.

### III-3. Optical properties

Fig. 3 shows the transmittance and absorbance spectra of ZnO thin films deposited at different bath temperatures (75 °C, 80 °C and 85 °C). The spectra revealed that the ZnO films have low absorbance in the visible region, which is a characteristic of ZnO. The transmittance decreases with increase in bath temperature. The transmittance edge was seen to be shifted slightly towards higher wavelength as the bath temperature was increased. This shift indicates decrease in band gap, which can be attributed to increase in the thickness and in grain size with bath temperature. Also Fig. 3(a) shows the occurrence of peaks in the absorbance (transmittance) plot at 358 nm. These peaks are attributed to the formation of excitons in ZnO thin films, by bath temperature, which decreased with decreasing the bath temperature. This last parameter influences a shift between the spectra, which means the decrease of band gap energy. Similar

peaks were obtained by other authors [28,29] after annealing of ZnO thin films.

The ZnO is a wurtzite structure semiconductor with direct band gap of 3.3 eV. The band gap was estimated using the Tauc's relationship [30] between the absorption coefficient,  $\alpha$ , and the photon energy,  $h\nu$ , using

$$\alpha h\nu = A(h\nu - E_g)^n \quad (6)$$

Where  $n = \frac{1}{2}$  for direct allowed transitions and  $n = 2$

for allowed indirect transitions. This equation gives the values of direct and indirect band gap ( $E_g$ ), when straight portion of  $(\alpha h\nu)^2$  against  $h\nu$  plot and

$(\alpha h\nu)^{\frac{1}{2}}$  as plotted against  $h\nu$  plot, and extrapolated to  $\alpha = 0$ . Fig. 4 shows the linear part of  $(\alpha h\nu)^2$  versus  $h\nu$  for ZnO film. From Fig. 4 the band gap was found to be 3.27 eV.

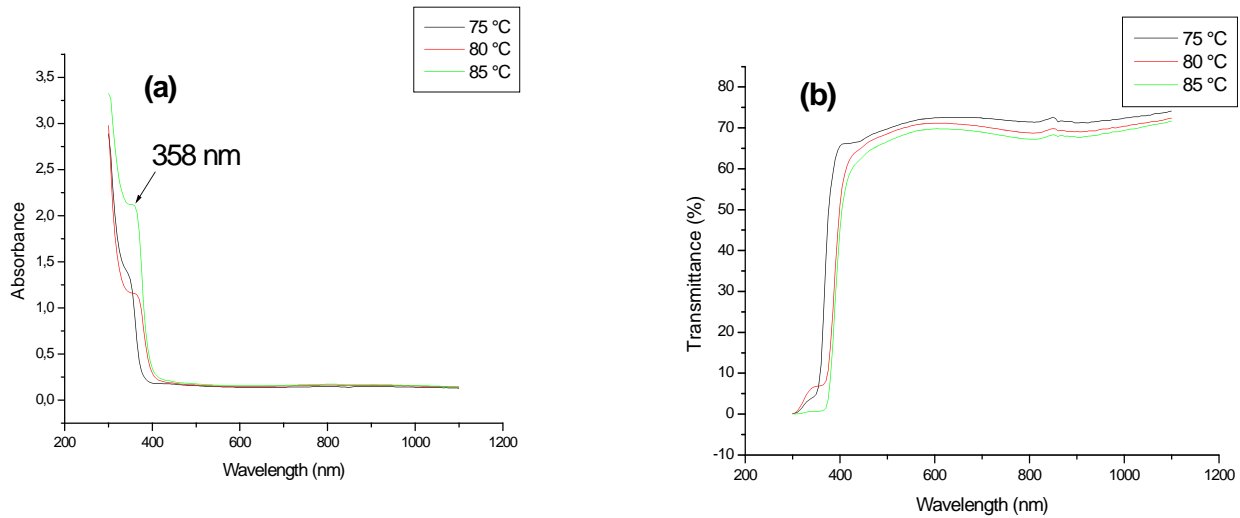


Fig. 3. Absorbance and Transmittance spectra of ZnO thin films deposited in the same conditions, and at different temperatures  $T = 75^{\circ}\text{C}$ ,  $80^{\circ}\text{C}$  and  $85^{\circ}\text{C}$ .

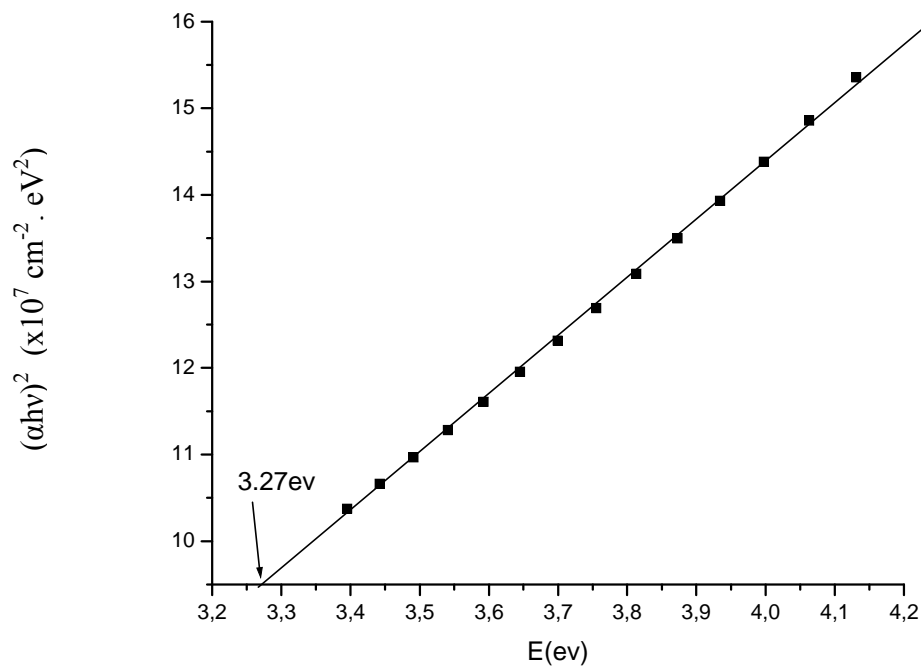


Fig. 4. Determination of the band gap of a ZnO thin film deposited on glass substrates from a basic solution ( $\text{pH}=10.47$ ), immersion time: 30 s, number of cycles: 20 and bath temperatures:  $80^{\circ}\text{C}$ .

#### IV. Conclusion

In this paper, we deposited the zinc oxide thin films by SILAR method from an aqueous solution of zinc sulphate. We discussed the classification of compounds which can be chemically deposited. And we studied the influence of some parameters of SILAR

technique such as: bath temperature, pH and substrate on the quality of our films. The XRD patterns showed formation of polycrystalline ZnO. SEM micrographs revealed ZnO films can be takes many shapes: needles, nanorods, nanoprisms, spindles, flower-like and hexagonal structures. The optical direct band gap decreases with increasing bath temperature.

## V. References

- [1] R. R. Potter, solar cells 16 (1986) 521.
- [2] S. C. Ko, Y. C. Kim, S. S. Lee, S. H. Choi, S. R. Kim, Sens. Actuators, A 103 (2003) 130.
- [3] D. H. Yoon, G. M. Choi, Sens. Actuators, B 45 (1997) 251.
- [4] D. Fernández-Hevia, J. de Frutos, A. C. Caballero, J. F. Fernández, Appl. Phys. Lett. 82 (2003) 212.
- [5] D. M. Bagnall, Y. F. Chen, Z. Zhu, T. Yao, S. Koyama, M. Y. Shen, T. Goto, Appl. Phys. Lett. 70 (1997) 2230.
- [6] R. L. Hoffman, B. J. Norris, J. F. Wager, Appl. Phys. Lett. 82 (2003) 733.
- [7] W. -T. Chiou, W. -Y. Wu, J. -M. Ting, Diam. Relat. Mater. 12 (2003) 1841.
- [8] S. C. Lyu, Y. Zhang, H. Ruh, H. -J. Lee, H. -W. Shim, E. -K. Suh, C. J. Lee, Chem. Phys. Lett. 363 (2002) 134.
- [9] J. -J. Wu, S. -C. Liu, J. Phys. Chem. B 106 (2002) 9546.
- [10] Y. G. Wang, C. Yuen, S. P. Lau, S. F. Yu, B. K. Tay, Chem. Phys. Lett. 377 (2003) 329.
- [11] J. Q. Hu, X. L. Ma, Z. Y. Xie, N. B. Wong, C. S. Lee, S. T. Lee, Chem. Phys. Lett. 344 (2001) 97.
- [12] M. L. de la Olvera, A. Maldonado, R. Asomoza, M. Meléndez-Lira, Sol. Energy Mater. Sol. Cells 71 (2002) 61.
- [13] J. L. Van Heerden, R. Swanepoel, Thin Solid Films 299 (1997) 72.
- [14] M. Fahoume et al, Sol. Energy Mater. Sol. Cells 90 (2006) 1437-1444.
- [15] H. M. Pathan, C. D. Lokhande, Bull. Mater. Sci. 27 (2004) 85.
- [16] A. Jimenez-Gonzalez, P. K. Nair, Semicond. Sci. Technol. 10 (1995) 1277.
- [17] A. Jimenez-Gonzalez, R. Suarez-Parra, J. Cryst. Growth 167 (1996) 649.
- [18] P. Kofstad, Nonstoichiometry, Diffusion and Electrical Conductivity in Binary Metal Oxides (Krieger, Malabar, FL, 1983) Ch. 1, p. 7.
- [19] F. H. Kroeger and H. Vink, in: Solid State Physics, Vol. 3, Eds. F. Seitz and D. Turnbull (Academic Press, New York, 1956) Ch. 2, p. 397.
- [20] P. S. Kumar and al./ Applied Surface Science 255 (2008) 2382-2387.
- [21] B. Cheng, E. T. Samulski, Chem. Commun. 8 (2004) 986.
- [22] B. Liu, H. C. Zeng, Langmuir 20 (2004) 4196.
- [23] D. Vernardou et al./ Thin Solid Films 515 (2007) 8764-8767.
- [24] Q. C. Li, V. Kumar, Y. Li, H. T. Zhang, T. J. Marks, R. P. H. Chang, Chem. Mater. 17 (2005) 1001.
- [25] J. P. Liu, X. T. Huang, Y. Y. Li, J. X. Duan, H. H. Ai, Mater. Chem. Phys. 98 (2006) 523.
- [26] J. P. Liu, X. T. Huang, Y. Y. Li, J. X. Duan, H. H. Ai, L. Ren, Mater. Sci. Eng. B 127 (2006) 85.
- [27] J. P. Joliet, J. Livage, et M. Henry. De la solution à l'oxyde, 1994.
- [28] F. Ren, C. Z. Jiang, X. H. Xiao, Nanotechnology 18 (2007) 4, 285609.
- [29] A. Ghosh et al. Journal of Alloys and Compounds 469 (2009) 56-60.
- [30] J. Tauc, R. Grigorovici, A. Vancu, Phys. Status Solidi 15 (1966) 627.